RSC Advances

ROYAL SOCIETY OF CHEMISTRY

www.rsc.org/advances

Graphical Abstract

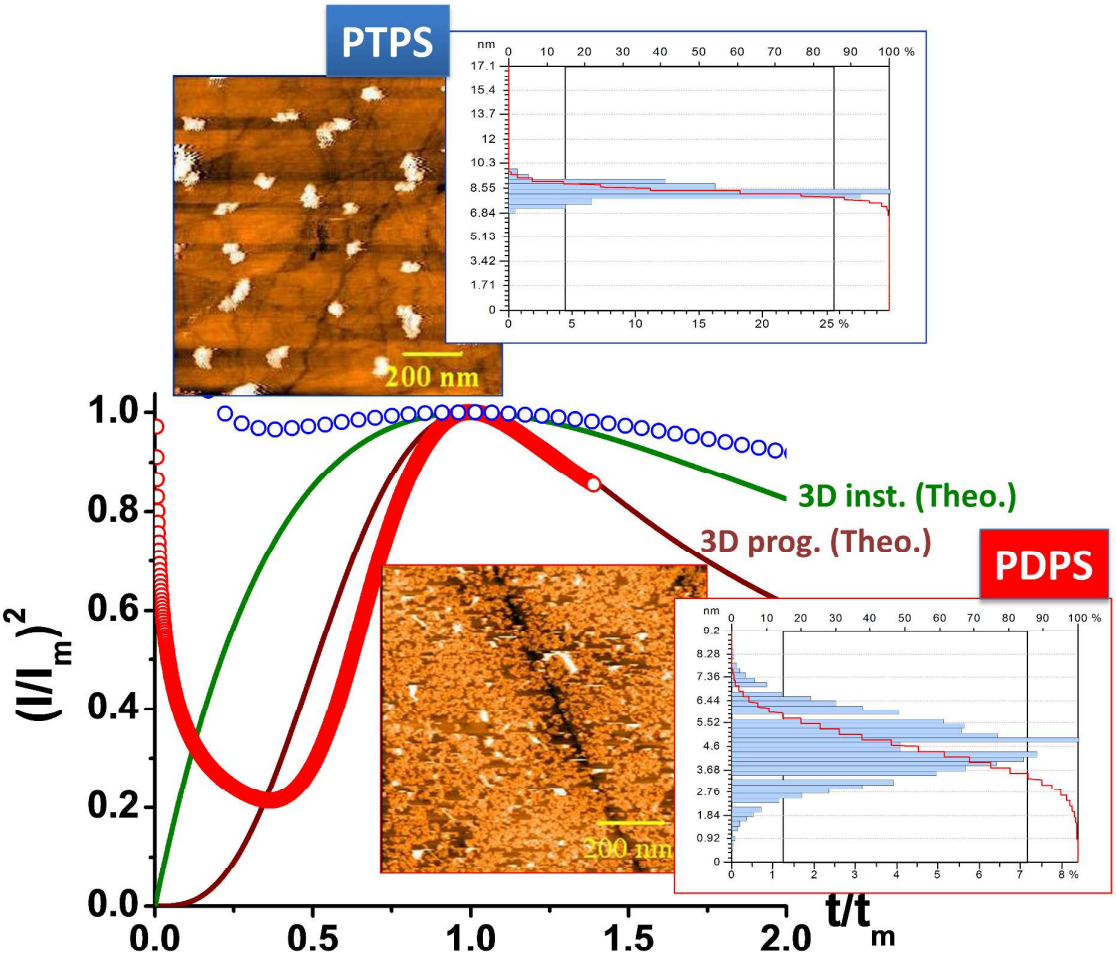

Cite this: DOI: 10.1039/c0xx00000x

www.rsc.org/xxxxxx

COMMUNICATION

The prospective of potentiostatic triple pulse strategy for template-free electrosynthesis of metal nanoparticles†

Saurav K. Guin[a] and Suresh K. Aggarwal*[a]

Received (in XXX, XXX) Xth XXXXXXXXX 20XX, Accepted Xth XXXXXXXXX 20XX

DOI: 10.1039/b000000x

Electrosynthesis of metal nanoparticles of controlled size and dispersion is a challenging task on a macrodisk electrode in the absence of any chemical or physical template. A potentiostatic triple pulse strategy (PTPS) was designed for the electrosynthesis of monodispersed lead nanoparticles (PbNPs) on glassy carbon electrode and the result was compared to the conventional potentiostatic double pulse strategy (PDPS). A switchover of the nucleation mechanism from progressive in PDPS to instantaneous in PTPS was observed for the first time during the final controlled growth step and this resulted in smaller and better monodispersed PbNPs (~8±2 nm).

Electrosynthesis is one of the promising techniques for preparing supported metal nanoparticles of controlled size, shape, crystallographic orientation, mass, thickness and morphology which are important for many applications including diamagnetic fluctuations. Lead nanoparticles (PbNPs) of size less than 87 nm can be employed as superconducting materials to study the quantum size effect on the superconducting properties[1] as well as zero-dimensional fluctuation diamagnetism. [2] Guin et al. reported the preparation of capped hemispherical PbNPs on a template free gold (Au) electrode at room temperature from the aqueous solution of 1 mM $Pb(ClO_4)_2$ in 0.1 M $HClO_4$.[3] A potentiostatic triple pulse strategy (PTPS), very different from the strategy developed by Adzic et al and Guin et al, [4,5] was first time introduced in that work and the variation of particle size as well as size dispersion with the pulse potentials and durations were reported. The heights of the capped hemispherical PbNPs varied from 2-18 nm, while lateral size (i.e. chord of NPs) varied in the sub-micron ranges. Henceforth, we would express the average height of NPs and the variation (i.e. range) of the heights of NPs by the terms "size" and "size dispersion", respectively. The wider size dispersion is termed as "polydisperse" while, the narrower size dispersion tends to be called as "monodisperse". It is interesting to note that the reason behind the considerable improvement in the particle size and size dispersion in PTPS compared to conventional potentiostatic double pulse strategy (PDPS) is not well understood. Gold could be a suitable substrate for the electrodeposition of lead, as the interaction energy of Pb with Au is much stronger than the interaction energies of Pb with Pb and Au with Au. However, to understand the importance of the pulse strategy, the influence of substrate could be removed. From this aspect, glassy carbon (GC) provides a low surface energy conductive substrate and exhibits weak metal-substrate interaction. The nucleation of lead on GC has been investigated for decades by single potentiostatic pulse; [6] but here we report firstly that the number of potentiostatic pulse and its potentials and sequences have great influence on the mechanism of electrocrystallization as well as in the particle size and size dispersion.

The working solution of 1 mM $Pb(ClO_4)_2$ in 0.1 M $HClO_4$ was prepared from Metrohm standard aqueous lead ion solution (C_{Pb2+} = 0.1000 ± 0.0005 M), 60% $HClO_4$ and Millipore-MilliQ water. After purging the working solution with high purity nitrogen for a minimum duration of 15 minutes, electrochemical experiments were carried out at room temperature with Autolab PGSTAT-30 electrochemical workstation controlled by GPES software by employing a three electrode voltammetric cell having glassy carbon (GC) working electrode (area = 0.071 cm^2), platinum wire counter electrode and Ag/AgCl(saturated) reference electrode. All the potentials are reported with respect to Ag/AgCl(saturated) reference electrode. The polishing of electrode in between the experiments was carried out by following standard protocol.[5] The polishing of GC electrode in between the experiments did not alter the overall activation and quality of the GC surface (Fig. S1, EIC). The PbNPs were characterized ex-situ by employing Nanosurf Easyscan 2 AFM by scanning with Silicon tip (CONTR-10) in contact static mode. The recorded AFM images were studied by the inbuilt programs of the Nanosurf Report 4.1 software in order to obtain the particle size histograms.

Fig. 1A shows the cyclic voltammogram of 1 mM $Pb(ClO_4)_2$ in 0.1 M $HClO_4$ on GC electrode at a scan rate of 10 mV s^{-1}. The potential scan starts from 0.4 V towards the cathodic direction. A surge of cathodic current starts from -0.49 V for the reduction of Pb(II)/Pb resulting in a cathodic peak at -0.58 V. In the reverse scan direction, two crossovers were observed at -0.55 V and -0.47 V between the forward and reverse scans. This characteristic nucleation loop suggests that the deposition of Pb(II) on GC has a nucleation overpotential, which is eventually the extra potential applied for nucleation over the thermodynamic equilibrium potential of Pb(II)/Pb(0). [7] Since, the activity of Pb(0) and GC in solid states are unity; thus the nucleation overpotential is an indirect measure of the kinetic hindrance of nucleation of Pb on GC than the nucleation of Pb on Pb. Therefore, GC does not provide any favorable interaction on Pb deposition i.e. Pb adatoms - adatoms interaction is stronger than the interaction of

Pd adatoms with the GC surface. Thus, nuclei of Pb are expected to be formed on GC followed by the three dimensional diffusion controlled growth. [8] At more positive potential, the anodic current increased due to the oxidation of the deposited Pb. A sharp anodic peak was observed with a peak potential at 0.41 V. It indicates that the anodic dissolution of the lead deposits is quite labile under the present experimental conditions. The open circuit potential (OCP, E_0) of the system was measured as -0.41 V, which is in agreement with the expected value (-0.40 V) calculated from the Nernst equation. [9] The open circuit potential or equilibrium potential, for the overall reaction at room temperature is given by Nernst equation: OCP = E_0 + 0.0295 log[Pb(II)]; where; E_0 = -0.312 V (vs. Ag/AgCl(saturated)), and [Pb(II)] is 0.001 M.

The mechanism of nucleation and growth of lead on GC by PDPS was studied by holding the potential of the electrode initially at +0.40 V (E_1) for 60 s (t_1) followed by a sharp change to a different potential (E_2) as indicated by the circles in Fig. 1A. The current transients were recorded at E_2 for a duration ranging between 10 - 70 s and are shown in Fig. 1B. No characteristic nucleation and growth feature was observed, except for the discharge current originated from the double layer molecular rearrangements within a few ms, for the current transients recorded upto 70 s at -0.15, -0.3, -0.4 V. The cathodic current sharply decreased at very short time scale also at -0.49 V due to the rearrangement of electrolyte species at the electrode-electrolyte interface, but it slowly increased after an induction time for ~22 s. This is attributed to an increase in the overall electroactive area due to increase in the number of Pb nuclei and/or growth of Pb nuclei. The spherical diffusion zone around each nucleus grew with time and at time (t_m) 50.44 s corresponding to the current maximum (I_m; -8.4 µA), these spherical diffusion zones overlapped and mass transfer became linear to a planar surface. The change in diffusion regime led to a decrease in the current with time following Cottrell equation. The value of t_m decreased, but the value of I_m increased as E_2 became more cathodic. At E_2 = -0.62 V, the values of t_m and I_m were observed as 0.64 s and 49.2 µA, respectively. It indicates that the rate of reduction of Pb(II) on GC increased with increasing the cathodic overpotential. For E_2 = -0.64 and -0.70 V, no current maxima could be resolved in the experimental time frame due to the fast nucleation and fast change of diffusion regime to Cottrell behavior. No characteristics of 2D or 2D-2D type transients were observed in any case. The type of three dimensional multiple nucleation and diffusion controlled growth was qualitatively studied by the dimensionless plot of $(I/I_m)^2$ vs. t/t_m for two limiting cases viz. instantaneous and progressive nucleations by following Scharifker-Hills(SH) model (Equations 1,2) and are shown in Fig. 1C.

(Here Equation 1 will be included)

(Here Equation 2 will be included)

It is important to mention that the quantitative evaluation of the electrocrystallization parameters from the SH model is undisputedly sensitive and controversial.[10-12] However, it is still being used in the electrodeposition community for a qualitative understanding of the early stage of nucleation and growth.[13-15] It could be inferred from Fig. 1C that at E_2= -0.49 V, the nucleation and growth was progressive i.e. new nuclei being continuously formed at low nucleation rate during the whole process of deposition. As the cathodic overpotential increased to -0.62 V, the nucleation and growth tended towards the instantaneous i.e. all the nuclei being immediately created at high nucleation rate and the number of nuclei remained constant during the growth process. From our present understanding, we anticipated that the nucleation and growth of Pb nuclei would be instantaneous at E_2 = -0.7 V. Here, we have not put any effort to extract the nucleation parameters from the current transients by Scharifker – Mostany (SM); Sluyters–Rehbach,Wijenberg, Bosco, Sluyters (SRWBS) and Heerman, Tarallo (HT) models; because our recent study revealed that no correlation exists in the nucleation parameters obtained from SH, SM, SRWBS, and HT models[10].

From the above mentioned analysis as well as with the experience gained from our earlier published report[3], we designed a similar PTPS strategy, where the first pulse (E_1) was fixed at 0.4 V for 60 s (t_1), followed by a short second pulse (E_2) at -0.7 V for 0.1 ms (t_2) and then followed by a third pulse (E_3) at -0.49 V for 70 s (t_3). The current transient was recorded during the third pulse and shown in Fig. 2A (i). The current transient recorded during PDPS (ii) at -0.49 V (where E_2 for time t_2 was skipped) was also overlaid in Fig. 2A. The time for current maximum significantly decreased to 0.94 s in PTPS from 50.44 s in PDPS, though the maximum current did not change much (PTPS: -7.6 µA; PDPS: -8.4 µA). In PTPS, as t_2 increased from 0.1 ms to 1 ms, the t_m increased from 0.94 s to 34.1 s, though i_m did not change much (Fig. 2A(iii)). When the E_1 was changed to the OCP value (-0.4 V) keeping all other parameters constant, the t_m increased from 0.94 s to 42.1 s, though i_m did not change much (Fig. 2A (iv)). The dimensionless plots of $(I/I_m)^2$ vs. t/t_m (Fig. 2B) showed a crucial change in mechanism of nucleation and growth. The nucleation and growth of Pb nuclei at -0.49 V became instantaneous in PTPS (i), while it was predominantly progressive in PDPS (ii). Moreover, the domination of the instantaneous type of nucleation and growth decreased as t_2 became longer (iii). Similar behaviour was also observed while the E_1 was changed to the OCP value (-0.4 V) (iv).

The final surface topographies of the PbNPs/GC at the end of 70 s of the current transients (i-iv) are shown in Fig. 3. The instantaneous nucleation and growth of PTPS resulted into discrete and monodispersed (average size 8±2 nm) tapped hemispherical PbNPs (Fig. 3 A,B). However, the progressive nucleation and growth and prolonged induction time resulted in small, overlapped and polydispersed (average size 5±5 nm) PbNPs (Fig. 3 C,D). Moreover, in PTPS, on increasing the second pulse duration, the dispersity of the size of PbNPs increased (Fig. 3 E,F). It is interesting to note that both the size and dispersity in size of the PbNPs increased when the PTPS experiment was started from OCP (Fig. 3 G,H).

The difference between PTPS and PDPS in the mechanism of nucleation and growth as well as in the dispersion in particle size of PbNPs arose because of the presence of a very short nucleation pulse of high cathodic overpotential in between the start and growth pulses. In case of PDPS, when the potential is switched from 0.4 V to -0.49 V, the surface sites on GC got slowly activated during the prolonged induction period of ~22 s. Then nucleation and growth of PbNPs passed through slow progressive type of nucleation depending on the dynamics of activation-

deactivation of surface sites. In PTPS, an enormous number of surface sites activated in very short time scale, when the potential is switched from 0.4 V to -0.7 V. However, due to very short imposition time (0.1 ms) of this pulse, a large number of active sites remained unoccupied as well as the electrode-electrolyte interface remains in a non-steady state and thus while the potential was switched back to -0.49 V, instantaneous nucleation happened to these unoccupied active sites (the dissolution of the subcritical nuclei upon the potential transition replenishes the Pb(II) ions in the double layer). This mechanism is believed to squeeze the size dispersion of PbNPs. Again, the majority of the active sites became occupied on increasing the duration of the second pulse as well as the electrode-electrolyte interface attains a steady state; thus its influence on nucleation and growth became inferior at the third pulse. That is why the dispersion in the particle size comparatively increased on increasing the duration of the second pulse. The start potential is crucial to restrict the irregular nucleation and growth of the pre-adsorbed Pb(II) on the GC surface. At OCP, a sufficient amount of Pb(II) ions got adsorbed at the oxygenated functionalities on GC surface and its irregular nucleation and growth throughout the three pulses resulted into the large particle size distribution and overlapped particles.

Therefore, the better monodispersity in the particle size could be achieved by the PTPS because of the controlled nucleation and growth at the final (the third) pulse step. The history of the GC surface, just before the final pulse, was created by the controlled activation and nucleation during the first and second pulses, respectively. However, Fig. 3 shows some aggregates of the PbNPs. It is important to note that the active sites are randomly distributed on the electrode in the absence of any physical or chemical templates. Therefore, it is still challenging to avoid particle coalescence by the potentiostatic pulse strategies on a template-free substrate.[5] However, the discrete particles could be formed by the multiple galvanostatic pulse strategy on a template-free electrode.[5]

Conclusions

The above discussed results not only unlash, for the first time, the cause of improvement in the particle size and size dispersion in PTPS compared to PDPS, but also show a prospective of PTPS for template-free electrosynthesis of metal nanoparticles. The potential of the start (first) pulse is important to restrict the irregular nucleation and growth of the pre-adsorbed ions on the electrode surface and OCP is not ideal for the start potential. The potential and duration of the seed (second) pulse are the most important features of the PTPS as it implements the number of unoccupied active sites to the following controlled growth pulse. The better monodispersity in the particle size could be achieved by the controlled nucleation and growth in the final (third) pulse with the pre-history effects of the first and second pulses on the GC surface. It can be noted that both thermodynamics and surface kinetics parameters (of both substrate and the deposited metals) play the key role in the electrochemical nucleation and growth of metal nanoparticles on the substrate. Therefore, the present work is expected to motivate detailed investigations of the thermodynamics and surface kinetics of PTPS for the electrosynthesis of metal nanoparticles. After an detailed investigation of the metal(deposited)-substrate pair, the PTPS could also be applicable to other metals than Pb. Further, the critically designed PTPS can electrochemically produce discrete and monodispersed capped hemispherical metal nanoparticles on a low surface energy conductive substrate. This study would be useful for designing systems of controlled size for fundamental studies and practical purposes in the field of material sciences and condensed-matter physics.

Notes and references

[a] *Fuel Chemistry Division, Bhabha Atomic Research Centre, Trombay, Mumbai - 400 085, India. Fax: +91-22-2550-5151; Tel: +91-22-2559-3740; E-mail: skaggr2002@gmail.com*

†*Electronic Supplementary Information (ESI) available: Fig. S1 The cyclic voltammograms of 5 mM $K_3[Fe(CN)_6]/K_4[Fe(CN)_6]$ in 0.1 M KCl at GC electrode polished in between the experiments. See DOI: 10.1039/b000000x/*

1. W.-H. Li, C.C. Yang, F.C. Tsao, K.S. Lee, *Phys. Rev. B*, 2003, **68**, 184507.
2. E. Bernardi, A. Lascialfari, A. Rigamonti, L. Romano, V. Lannotti, G. Ausanio, C. Luponio, *Phys. Rev. B*, 2006, **74**, 134509.
3. S.K. Guin, H.S. Sharma, S.K. Aggarwal, *Electrochim. Acta*, 2010, **55**, 1245.
4. G.D. Adzic, D.M. Drazic, A.R. Despic, *J. Electroanal. Chem.*, 1988, **239**, 107.
5. S.K. Guin, J.S. Pillai, A.S. Ambolikar, A. Saha, S.K. Aggarwal, *RSC Adv.*, 2013, **3**, 17977.
6. F. Palmisano, E. Desimoni, L. Sabbatini, G. Torsi, *J. Appl. Electrochem.*, 1979, **9**, 517.
7. I. Danaee, *J. Ind. Eng. Chem.*, 2013, **19**, 1008.
8. X. Huang, Y. Chen, J. Zhou, Z. Zhang, J. Zhang, *J. Electroanal. Chem.*, 2013, **709**, 83.
9. Y. Zhao, F.-X. Deng, L.-F. Hua, Y.-Q. Liua, G.-B. Pana, *Electrochim Acta*, 2014, **130**, 537.
10. S.K. Guin, R. Phatak, J.S. Pillai, A. Sarkar, S.K. Aggarwal; Communicated to *RSC Advances*, RA-ART-05-2014-005159.
11. A. Milchev, L. Heerman, *Electrochim. Acta*, 2003, **48**, 2903.
12. L. Komsiyska, G. Staikov, *Electrochim. Acta*, 2008, **54**, 168.
13. R.-W. Tsai, Y.-T. Hsieh, P.-Y. Chen, I.-W. Sun, *Electrochim. Acta*, 2014, **137**, 49.
14. J. Xu, G. Yua, B. Hub, J. Zhang, Q. Dong, X.Y. Zhang, *Powder Technol.*, 2014, **264**, 561.
15. A.G. Oshchepkov, A.N. Simonov, P.A. Simonov, A.N. Shmakov, N.A. Rudina, A.V. Ishchenko, O.V. Cherstiouk, V.N. Parmon, J. *Electroanal. Chem.*, 2014, **729**, 34.

Fig. 1

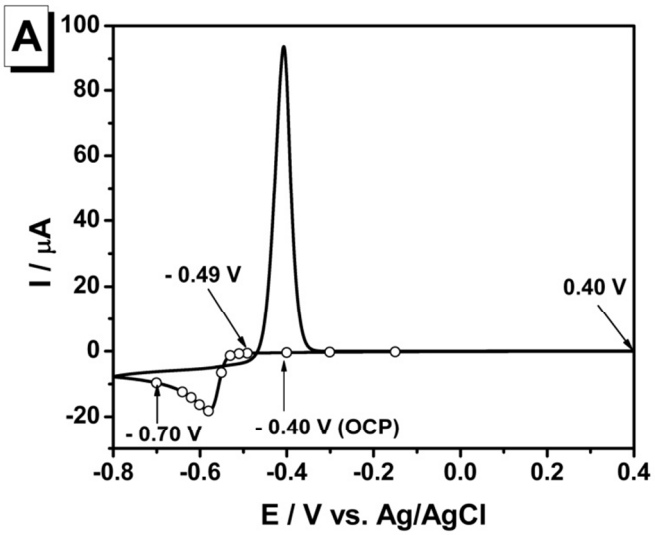

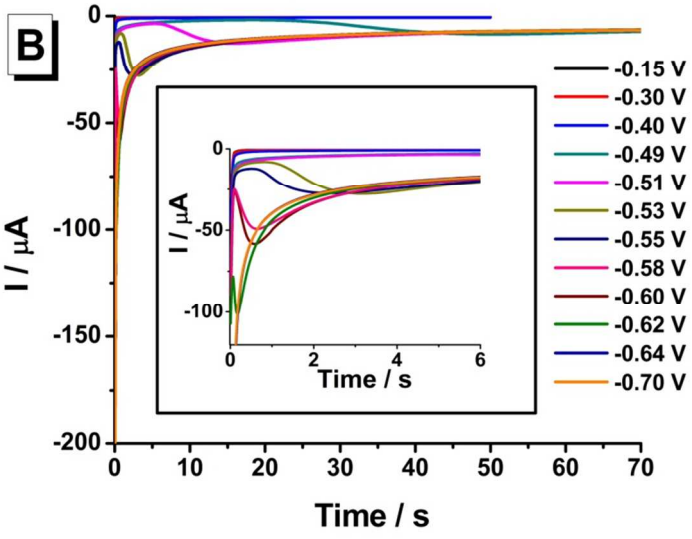

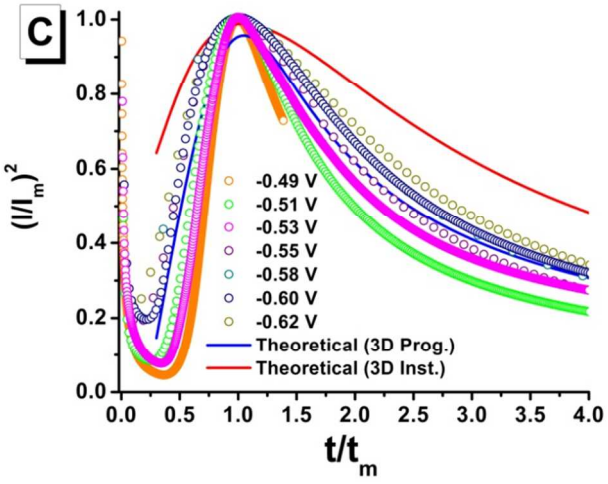

Fig. 2

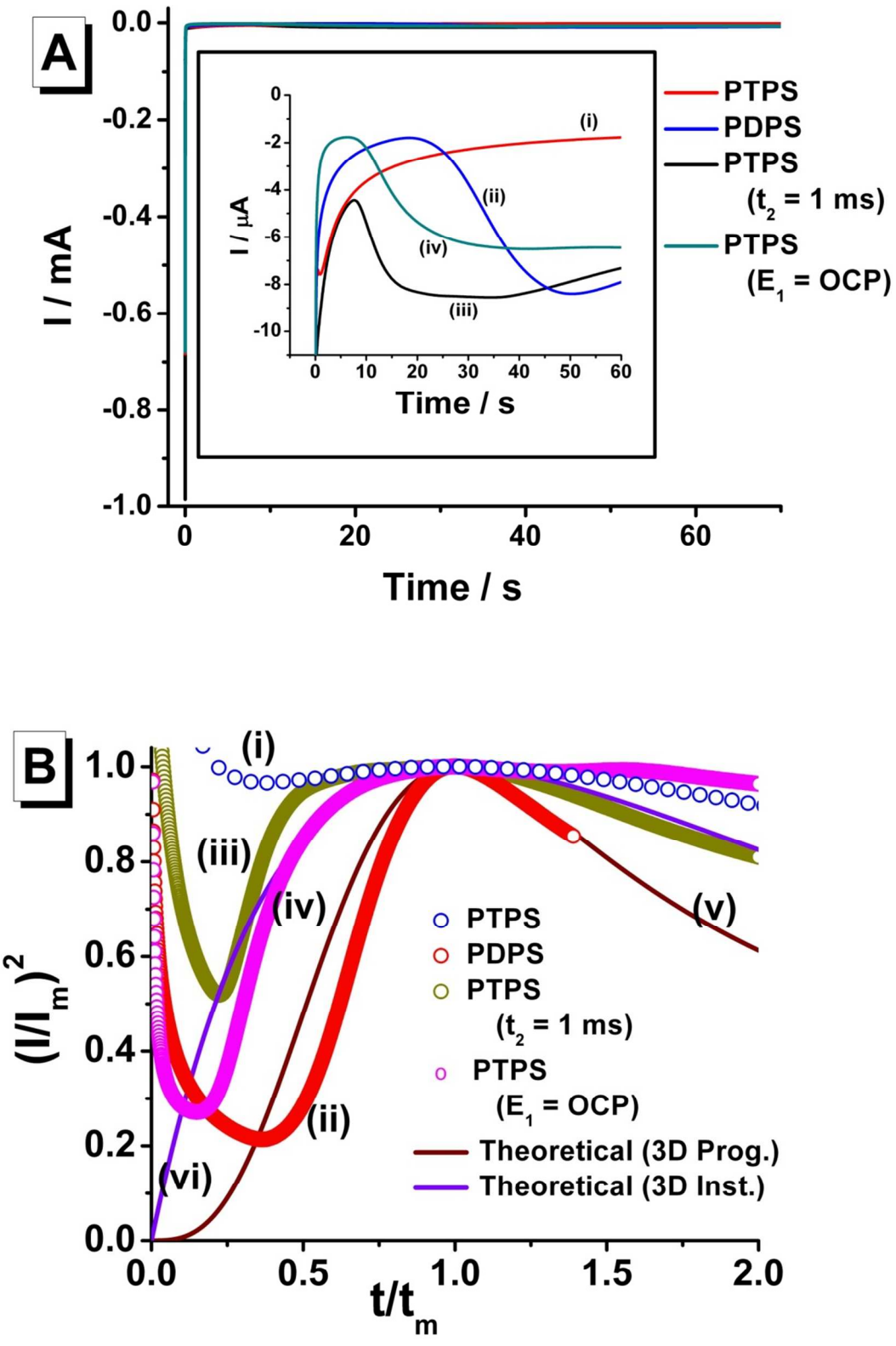

Fig. 3

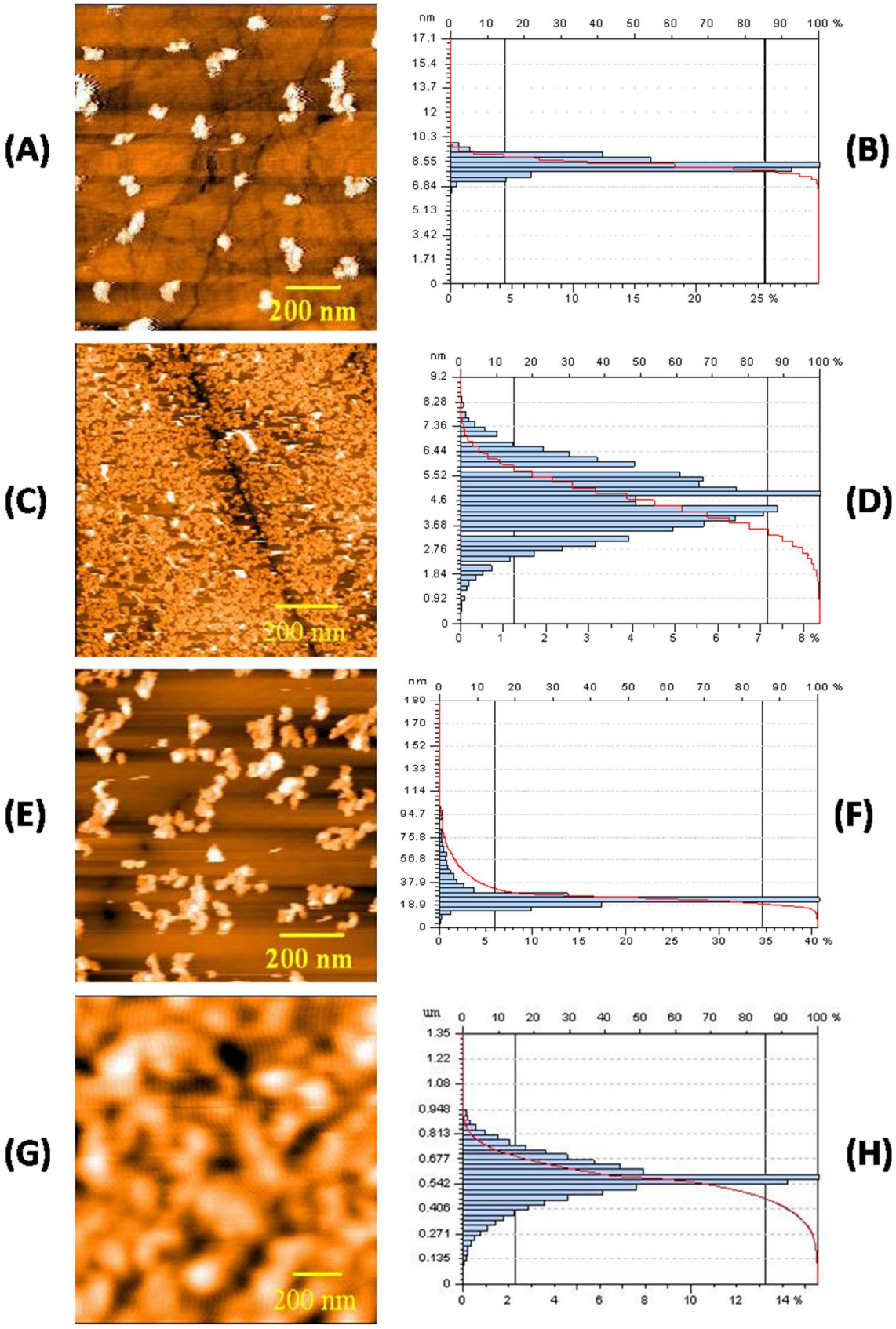

Figure Captions

Fig. 1 (A) Cyclic voltammogram of 1 mM $Pb(ClO_4)_2$ in 0.1 M $HClO_4$ on GC electrode at a scan rate of 10 mV s^{-1}. **(B)** Chronoamperograms recorded at -0.15, -0.30, -0.40, -0.49, -0.51, -0.53, -0.55, -0.58, -0.60, -0.62, -0.64 and -0.70 V; Preceded pulse: E_1 = 0.4 V, t_1 = 60 s. **(C)** The dimensionless plot of $(I/I_m)^2$ vs. t/t_m along with the theoretical curves for instantaneous and progressive nucleation according to SH model.

Fig. 2 (A) Chronoamperograms recorded at -0.49 V for 70 s for (i) PTPS (Preceded pulses: E_1 = 0.4 V, t_1 = 60 s, E_2 = -0.7 V, t_2 = 0.1 ms), (ii) PDPS (Preceded pulse: E_1 = 0.4 V, t_1 = 60 s), (iii) PTPS (Preceded pulses: E_1 = 0.4 V, t_1 = 60 s, E_2 = -0.7 V, t_2 = 1 ms); (iv) PTPS (Preceded pulses: E_1 = -0.4 V, t_1 = 60 s, E_2 = -0.7 V, t_2 = 0.1 ms). **(B)** The dimensionless plot of $(I/I_m)^2$ vs. t/t_m along with the theoretical curves for instantaneous and progressive nucleation according to SH model.

Fig. 3 The surface topographies (A,C,E,G) and particle size distributions (B,D,F,H) of PbNPs after **(A,B)** PTPS (E_1 = 0.4 V, t_1 = 60 s, E_2 = -0.7 V, t_2 = 0.1 ms, E_3 = -0.49 V, t_3 = 70 s), **(C,D)** PDPS (E_1 = 0.4 V, t_1 = 60 s, E_2 = -0.49 V, t_2 = 70 s), **(E,F)** PTPS (E_1 = 0.4 V, t_1 = 60 s, E_2 = -0.7 V, t_2 = 1 ms, E_3 = -0.49 V, t_3 = 70 s); **(G,H)** PTPS (E_1 = -0.4 V, t_1 = 60 s, E_2 = -0.7 V, t_2 = 0.1 ms, E_3 = -0.49 V, t_3 = 70 s).

Equations

$$\left[\frac{I}{I_m}\right]^2 = 1.9542\left(\frac{t}{t_m}\right)\left[1-\exp(-1.2564\left(\frac{t}{t_m}\right)\right]^2 \quad (1)$$

$$\left[\frac{I}{I_m}\right]^2 = 1.2254\left(\frac{t}{t_m}\right)\left[1-\exp\ (-2.3367\left(\frac{t}{t_m}\right)^2\right]^2 \quad (2)$$